Wetlands (2022) 42: 49
https://doi.org/10.1007/s13157-022-01565-3

COASTAL WETLANDS

Surface Elevation Change Dynamics in Coastal Marshes Along the Northwestern Gulf of Mexico: Anticipating Effects of Rising Sea-Level and Intensifying Hurricanes

Jena A. Moon[1] · Laura C. Feher[2] · Tiffany C. Lane[3] · William C. Vervaeke[2,4] · Michael J. Osland[2] · Douglas M. Head[5] · Bogdan C. Chivoiu[6] · David R. Stewart[7] · Darren J. Johnson[6] · James B. Grace[2] · Kristine L. Metzger[7,8] · Nicole M. Rankin[9]

Received: 14 May 2021 / Accepted: 9 May 2022 / Published online: 7 June 2022

Abstract
Accelerated sea-level rise and intensifying hurricanes highlight the need to better understand surface elevation change in coastal wetlands. We used the surface elevation table-marker horizon approach to measure surface elevation change in 14 coastal marshes along the northwestern Gulf of Mexico, within five National Wildlife Refuges in Texas (USA). During the 2014–2019 study period, the mean rate of surface elevation change was 1.96 ± 0.87 mm yr^{-1} (range: -1.57 to 8.37 mm yr^{-1}). Vertical accretion rates varied due to landscape proximity relative to sediment inputs from Hurricane Harvey. At most sites, vertical accretion offset subsurface losses due to shallow subsidence. However, net elevation gains were often lower than recent relative sea-level rise rates, and much lower than rates expected under future sea-level rise. Because these marshes are not keeping pace with recent sea-level rise, it is unlikely that they will be able to adjust to future accelerations. Climate change threatens these Texas coastal wetlands and the ecological and economic services they provide. By characterizing the status and prospective loss of coastal marshes, our study reinforces the value of identifying local and landscape-level adaptation mechanisms that can enhance the ability of coastal marshes to adapt to threats posed by climate change.

Keywords Surface elevation table · Texas · Hurricane Harvey · Elevation change · Coastal marsh · Gulf of Mexico

Introduction

Coastal wetlands provide critical ecosystem services, making them one of the most valuable ecosystems on the planet (Daily et al. 1997; Costanza et al. 2014). Coastal wetlands store carbon, support fisheries, improve water quality, provide wildlife habitat, protect coastal communities, and offer popular recreational opportunities (Barbier et al. 2011). However, due to their position at the land-sea interface, coastal wetlands are threatened by climate change (Kirwan and Megonigal 2013; Gabler et al. 2017; Osland et al. 2018). In particular, accelerated sea-level rise (Sweet

✉ Jena A. Moon
jena_moon@fws.gov

[1] U.S. Fish and Wildlife Service, 1035 Buccaneer Drive, Winnie, TX 77665, USA

[2] U.S. Geological Survey, Wetland and Aquatic Research Center, Lafayette, LA 70506, USA

[3] U.S. Fish and Wildlife Service, Florida Ecological Services, Jacksonville, FL 32256, USA

[4] National Park Service, 13165 Mt. Pleasant Rd., Jacksonville, FL 32225, USA

[5] U.S. Fish and Wildlife Service, 7950 S. Gulfway Drive, Sabine Pass, TX 77655, USA

[6] Cherokee Nations Systems Solutions, contracted to U.S. Geological Survey, Wetland and Aquatic Research Center, Lafayette, LA 70506, USA

[7] U.S. Fish and Wildlife Service, 500 Gold Ave SW, Albuquerque, NM 87103, USA

[8] U.S. Geological Survey, 1064 E. Lowell Street, Tucson, AZ 85721, USA

[9] U.S. Fish and Wildlife Service, 1875 Century Blvd NE, Atlanta, GA 30345, USA

et al. 2017) and hurricane intensification (Kossin et al. 2017; Seneviratne et al. 2021) threaten coastal wetlands and the ecosystem services they provide. Maintaining and enhancing the ecological and economic contributions of coastal wetlands in the face of climate change requires information regarding surface elevation change dynamics, as these dynamics underpin the stability of wetland ecosystems. In this communication, we examine surface elevation change within coastal marshes in Texas along the northwestern Gulf of Mexico coast (USA; Fig. 1).

Coastal wetlands are resilient ecosystems that have the potential to build elevation to adjust to moderate rates of sea-level rise via positive feedbacks between inundation, plant growth, and sedimentation (Morris et al. 2002; Woodroffe et al. 2016). However, higher rates of sea-level rise can overwhelm the ability of coastal wetlands to build elevation, leading to wetland loss due to conversion to open water (Saintilan et al. 2020; Törnqvist et al. 2020). A striking example of wetland loss due to high rates of relative sea-level rise can be found in Louisiana where rates of coastal wetland loss have been high during the last century (Couvillion et al. 2017; Törnqvist et al. 2020). Altered hydrology, reduced sediment delivery, and high rates of erosion have prevented many coastal marshes in Louisiana from building sufficient elevation to counteract high rates of subsidence and relative sea-level rise (Blum and Roberts 2009; Day et al. 2000; Couvillion et al. 2017; Törnqvist et al. 2020). The Texas coast also experiences high rates of subsidence and relative sea-level rise, especially near the Louisiana border (Sweet et al. 2017). When compared to Louisiana, wetland loss (i.e., wetland conversion to open water) and surface elevation dynamics within coastal wetlands in Texas have not been as thoroughly investigated (Cahoon et al. 2004; Cahoon et al. 2011; McKee and Grace 2012; Swanson 2020; Cressman 2020; see also regional inventory in Osland et al. 2017).

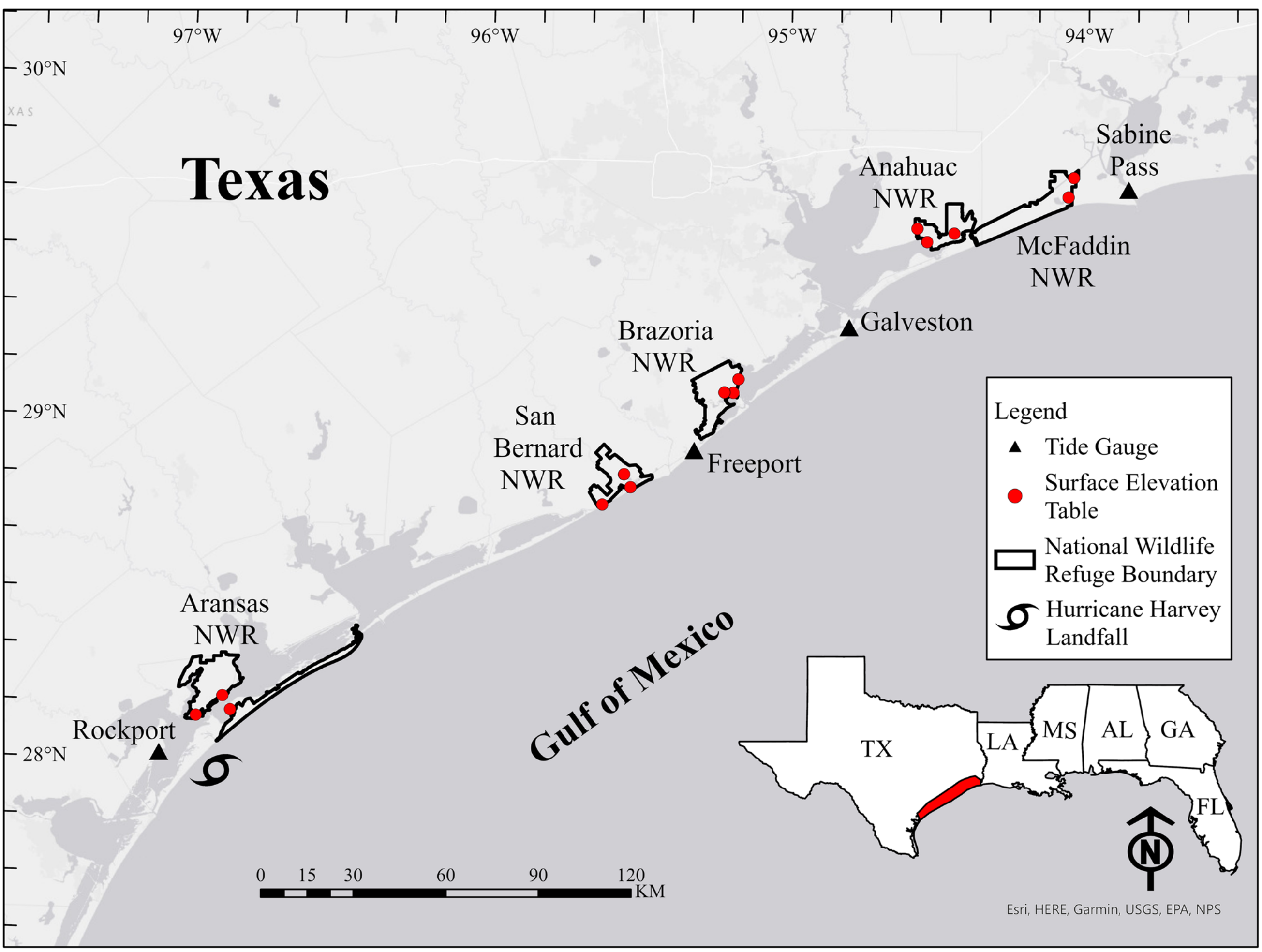

Fig. 1 Map showing the locations of the 14 coastal marsh surface elevation change study sites within five coastal Texas National Wildlife Refuges (USA). Hurricane Harvey landfall is shown with a hurricane symbol. NWR = National Wildlife Refuge; SET-MH = surface elevation table – marker horizon

Beyond accelerated sea-level rise (Sweet et al. 2017), coastal wetlands in the northwestern Gulf of Mexico are also highly vulnerable to hurricanes. In the coming century, global warming is expected to increase the frequency of the most intense hurricanes (i.e., major hurricanes), increase rainfall rates produced by hurricanes, increase the poleward distribution of hurricanes, and increasingly lead to the rapid intensification of hurricanes (Kossin et al. 2017; Seneviratne et al. 2021). The effects of hurricanes on wetland surface elevation change are variable and often hurricane specific (Cahoon 2006; Krauss and Osland 2020). Intense storms have the potential to lead to vegetation dieback, peat collapse, and conversion of wetlands to open water (Cahoon et al. 2003; Osland et al. 2020; Stagg et al. 2021). However, hurricanes can also provide an important source of sediment and nutrients for coastal wetlands increasing elevation capital, and thereby enhancing their ability to adjust to sea-level rise (Cahoon et al. 1995a; Feher et al. 2020; McKee et al. 2020). In the face of hurricane intensification, there is a need to advance understanding of the effects of hurricanes on wetland surface elevation dynamics.

This study was conducted within 14 coastal marsh sites located within five National Wildlife Refuges along the northwestern Gulf of Mexico (USA; Fig. 1). Hurricane Harvey affected this area in 2017, enabling us to also investigate hurricane effects on wetland surface elevation change. We specifically investigated the following questions: (1) How do rates of surface elevation change, vertical accretion, and subsurface change vary in Texas coastal marshes within five National Wildlife Refuges?; (2) What are the effects of Hurricane Harvey on marsh vertical accretion and surface elevation change?; and (3) How do rates of surface elevation change in coastal marshes compare with recent and expected future rates of relative sea-level rise? Collectively, the data and information from this study build foundational knowledge to better anticipate and prepare for coastal wetland responses to accelerating sea-level rise and intensifying hurricanes.

Methods

Study Area

We conducted this study within the following five National Wildlife Refuges (NWR) spanning an approximate 360-km section of the Texas coast (USA): Aransas, San Bernard, Brazoria, Anahuac, and McFaddin (listed in geographic order from south to north; Fig. 1). The area has a humid, subtropical climate with a strong maritime influence. The tides along this coastline are microtidal, mixed diurnally and semidiurnally, generally ranging from 30–60 cm (NOAA 2019a). The mean annual precipitation ranges from 1010 to 1360 mm, and the mean growing season length is 250 days (NOAA 2019b). Coastal wetlands in the northern portion of the study area receive more precipitation and freshwater inputs than the south, which results in lower salinities in the north and much higher salinities (i.e., hypersaline conditions) in the south (Longley 1994, 1995; Osland et al. 2014, 2016, 2019). Thus, the northern marshes are more productive (Gabler et al. 2017; Osland et al. 2018) and dominated primarily by grass-like plants including *Spartina patens*, *Spartina spartinae*, *Bolboschoenus robustus*, *Schoenoplectus americanus*, and *Distichlis spicata* (Table 1). In contrast,

Table 1 Descriptions for each of the 14 coastal marsh sites within the five coastal Texas National Wildlife Refuges (USA). In the vegetation column, plant species are listed in order of dominance

Refuge	Site	Site abbreviation	Dominant vegetation[1]
Aransas	Aransas-Intracoastal Waterway	AR-ICWW	BAMA, MOLI, SADE
	Matagorda Island	MI	SPAL, BAMA
	Blackjack	BJ	DISP, SPAL, BAMA
San Bernard	San Bernard-Barrier Island	SB-BI	BAMA, SPAL
	San Bernard-Intracoastal Waterway	SB-ICWW	DISP, BAMA, SPAL
	Cow Trap	CT	DISP, BAMA
Brazoria	Brazoria-Barrier Island	BR-BI	BAMA, SADE, AVGE, SPAL
	Alligator Lake	AL	DISP, BAMA,
	North Peninsula	BNP	BAMA, DISP
Anahuac	Alice Jackson White	AJW	SCRO, DISP
	Yellow Rail	YR	SPSP, SPPA, DISP
	Jackson Ditch	JD	SPPA
McFaddin	Willow-Barnet	WB	SPPA, SCRO
	10 Mile Cut	10MC	SPPA

[1]Species abbreviations: AVGE = *Avicennia germinans*, BAMA = *Batis maritima*, DISP = *Distichlis spicata*, MOLI = *Monanthochloe littoralis*, SADE = *Salicornia depressa*, SCRO = *Scirpus robustus*, SPAL = *Spartina alterniflora*, SPPA = *Spartina patens*, SPSP = *Spartina spartinae*

the higher salinity regimes in the southern marshes lead to an increase in coverage of succulents and salt-tolerant plants, including *Batis maritima*, *Salicornia depressa*, *Salicornia bigelovii*, *Monanthochloe littoralis*, and *Borrichia frutescens* (Table 1) (Dunton et al. 2001; Gabler et al. 2017; Osland et al. 2019; Stagg et al. 2021). Across much of the study area, *Spartina alterniflora* occupies the lowest and most inundated tidal saline wetland zones (Rasser et al. 2013; Gabler et al. 2017; Stagg et al. 2021). The study area spans a tropical-temperate transition zone where extreme freeze events are sporadic, occurring once every two to three decades (Osland et al. 2021). These freeze events govern the northern range limit of mangrove forests, which are freeze-sensitive (Sherrod and McMillan 1985; Armitage et al. 2015; Weaver and Armitage 2018). Sparse and freeze-stunted black mangrove individuals (*Avicennia germinans*) are present near and within several of the sites (e.g., Aransas, San Bernard, Brazoria).

Site Selection

We used the U.S. Fish and Wildlife Service (USFWS) National Cadastral Layer along with marsh habitat data from Enwright et al. (2015) to limit our area of interest to only intermediate, brackish, and salt marshes within the five NWRs. We generated a labeled 0.5-ha fishnet over each NWR and then randomly selected marsh locations for site visits. Field evaluations were necessary because the resolution of available geospatial data are often too imprecise for final determination of the suitability of a given sampling location. Initial site visits were conducted between June and August 2013. Upon arrival at a random field location, the site was evaluated to ensure it met study criteria. These criteria included: 1) site located in a tidal marsh with uniform vegetation community and cover dominated by graminoid or succulent vegetation; 2) site without obvious signs of disturbance (e.g., trampling and other vegetation impacts from disturbance); 3) site at least 25 m from nearby waterbodies; 4) sites required to be at least 25 m away from and have minimal influence from spoil banks, levees, roads, or any other human-induced landscape alteration; and 5) sites required to have reasonable access via airboat, boat, truck, and/or foot. If a field site did not meet all of the five criteria, it was excluded from the study and the next random location was visited for assessment. Searches continued until the appropriate number of sites within each of the five NWRs were met.

Study Design and Surface Elevation Change Measurements

We measured changes in surface elevation at each of the five refuges using the SET-MH approach [surface elevation table (SET) – marker horizon (MH)] (Cahoon et al. 2002a, b; Callaway et al. 2013; Lynch et al. 2015; Cahoon et al. 2020). The SET is a portable mechanical leveling device providing repeated, high-resolution measurements of elevation change in wetland sediments or shallow water bottoms relative to the depth of a permanent benchmark that has been anchored into the soil until refusal. We installed deep rod SETs to depths ranging from 7.6 to 37.8 m (mean ± SE = 16.0 ± 1.9 m; Table S1). During measurements, the SET arm is attached to the permanent SET benchmark and extended over the marsh surface at four fixed positions. The SET arm is carefully leveled to rest horizontally to the ground, and each of nine fiberglass pins are lowered through the arm to the soil surface. The height of each pin above the arm is measured on repeated sampling events. Changes in the height of the pins between sampling events are used to quantify soil surface elevation change over time relative to the permanent benchmark (Cahoon et al. 2002a). Marker horizons are artificial soil layers (e.g., feldspar) established on the surface of wetland or shallow water bottoms to measure subsequent surface sediment accretion (Baumann et al. 1984; Cahoon and Turner 1989). Cores are taken with a soil corer from the soil surface to this layer on repeated sampling events, and the thickness of the sediment accumulated above the layer is measured as vertical accretion.

We measured surface elevation change at 14 sites across the five refuges (i.e., 2–3 sites per refuge; Table 1). In April 2014, we established three permanent SET-MH stations at each of the 14 sites, for a total of 42 SET-MH stations. Each station consisted of a single SET benchmark and three or more marker horizon plots. In 2019, orthometric height relative to the North American Vertical Datum of 1988 (NAVD 88) was determined for each benchmark using digital leveling in combination with repeated, overlapping static Global Positioning System (GPS) surveys (Table S2). The GPS surveys were post-processed with the National Geodetic Survey OPUS Projects service (Gillins et al. 2019). The orthometric height of each benchmark was then used to convert the SET-derived relative surface elevation change data from each sampling date to an orthometric marsh elevation in NAVD 88. Three feldspar marker horizon plots (0.25 m^2; 0.5 m by 0.5 m) were established in the immediate vicinity of each SET benchmark in April 2014, and three additional marker horizon plots were added to each benchmark in November 2017 following the landfall of Hurricane Harvey. We established the second set of marker horizons because the 2014 marker horizons had deteriorated at some sites and were no longer visible.

During each sampling event, surface elevation measurements were made for nine pins on four fixed measurement positions (compass bearings) around each benchmark, for a total of 36 elevation measurements per benchmark per sampling event. Vertical accretion was determined by measuring the depth to the feldspar layer within cores collected from each marker horizon (i.e., from the 2014 and/or 2017 marker horizons, where available), using a "mini-Macaulay" corer (custom fabrication, Nolan's Machine Shop, Lafayette, LA, USA), which cuts a core (2 cm) without vertical compression (McKee and Vervaeke 2018). Surface elevation dynamics at each SET-MH station were measured roughly twice per year across the 5.5-year period between June 2014 and December 2019 (i.e., 9–12 total SET sampling events per site). Vertical accretion at each SET-MH station was measured roughly once per year except for 2015 (i.e., 4–5 total MH sampling events per site).

Recent and Future Sea-level Rise (SLR) Rates

Recent SLR rates for each refuge were estimated using relative sea-level rates from nearby NOAA tide gauge stations (NOAA 2020) for the most recent tidal epoch (2001–2019). SLR rates derived from the most recent tidal epoch are hereafter referred to as recent tidal epoch-based SLR rates. We determined the recent tidal epoch-based rates with linear regressions applied to the monthly mean sea-level data with the average seasonal cycle removed, with the data provided by NOAA (2020).

Future projected relative SLR (RSLR) rates for the study area were estimated using alternative SLR scenarios produced by Sweet et al. (2017) for the 4$^{\text{th}}$ National Climate Assessment. We selected three global mean SLR scenarios (Intermediate-Low, Intermediate, and Intermediate-High), which respectively correspond to global mean SLR increases of 0.5 m, 1.0 m, and 1.5 m by 2100. To approximate the RSLR rate by 2100 for the study area under each of the three scenarios, we used the data provided by Sweet et al. (2017) to calculate RSLR rates for the 2090–2100 decade from the refuge-specific RSLR projections. We used the five refuge-specific RSLR rates to calculate the following range in RSLR rates for each of the three selected SLR scenarios for the 2090–2100 decade: 8–10, 19–22, and 34–36 mm yr^{-1}, respectively, for the Intermediate-Low, Intermediate, and Intermediate-High scenarios.

Hurricane Harvey

In August of 2017, Hurricane Harvey made landfall along the central coast of Texas, becoming the first major hurricane to impact the state since Hurricane Ike in 2008. Hurricane Harvey developed in the Gulf of Mexico, striking the Texas coast from a southeasterly direction, making landfall on San Jose Island near Rockport, Texas on 26 August 2017 as a Category 4 storm with sustained winds of 213 km/h (Blake and Zelinsky 2018). Storm surge depths during Harvey were estimated as 1.8 to 3.0 m within the back bays between Port Aransas and Matagorda and 0.6 to 1.2 m from Matagorda through the upper Texas coast (Blake and Zelinsky 2018). Hurricane Harvey was a slow-moving storm that produced heavy precipitation (> 1000 mm) and prolonged freshwater flooding in some areas (Blake and Zelinsky 2018). The combination of high storm surge and high surface water inputs produced dynamic patterns in the deposition of marine and/or terrigenous sediments in coastal marshes and estuaries (Du et al. 2019; Williams and Liu 2019; Yao et al. 2020; Kuhn et al. 2021). On the first sampling event following Harvey (November 2017), we measured the depth of deposited sediments left by Harvey within the same cores taken from the marker horizon plots. Within these cores, the sediments deposited by Hurricane Harvey were easily distinguished from surrounding soil layers by color, texture, and absence of fine roots (McKee and Cherry 2009; McKee et al. 2020).

Data Analyses: Data Organization and Preparation

Prior to all data analyses, we converted the pin-level SET data to station-level SET data. First, we subtracted the elevation reading of each individual pin on each sampling date from its initial value to determine cumulative elevation change (Lynch et al. 2015). The pin-level elevation change values for each measurement date were averaged to obtain the mean station-level data for each date. For the accretion data, we averaged the plot-level marker horizon data to obtain mean station-level marker horizon data (Lynch et al. 2015).

Data Analyses: Station-level Rates

Rates of surface elevation change derived from SET data (y) have historically been quantified from linear relationships using simple regression where it is assumed that observed y is a linear function of a parameter vector β. However, due in part to the effects of Hurricane Harvey, the elevation change patterns at our sites included a diverse combination of linear and nonlinear relationships (see panels in Figs. 2 and 3). Thus, generalized additive models (GAMs) that are more flexible than standard linear models were used to quantify rates of surface elevation change and vertical accretion for each of the 14 sites. Initially, we fit GAM models to each site using the general form given by

$$g(\mu_t) = \beta_0 + \sum_{i=1}^{n} f_j(X_j) + \varepsilon$$

where μ is the conditional mean related to a one-to-one function g, β_0 is the intercept term, X_j is the main effect of station and a penalized thin-plate regression spline term for the interaction between time and station (i.e., factor-smooth interaction term), ε is the random residual error, and $\sum_{i=1}^{n} f_j(X_j)$ are smoothers of covariates. Each smoother is

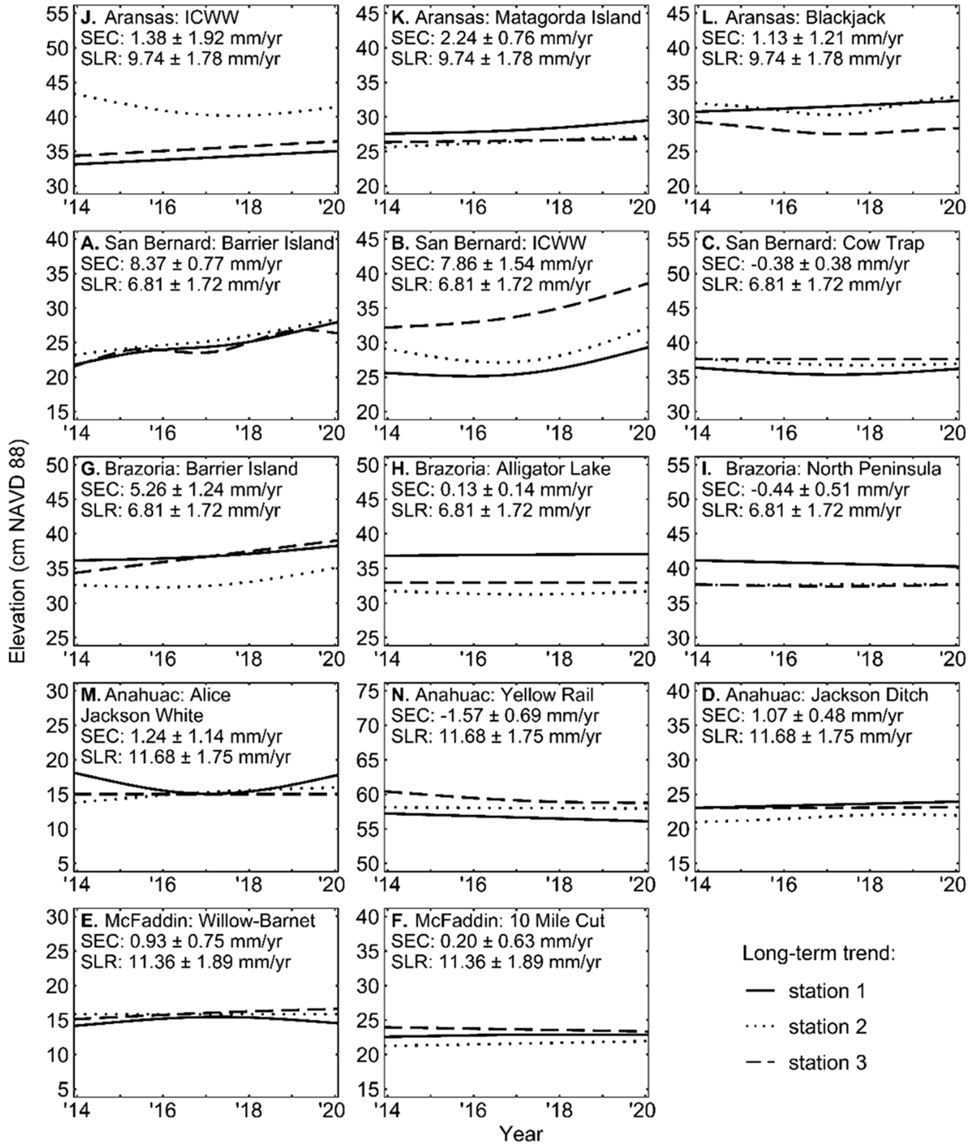

Fig. 2 Surface elevation change from the SETs (surface elevation tables) at the 14 coastal marsh sites. Generalized additive model-based results for each station at each site are presented in panels as black lines. Values in the plot labels represent the site-level rates of surface elevation change (SEC) and recent sea-level rise 2001–2019 (SLR) (mean ± standard error). Note that while elevation on the y-axis is presented in centimeters (cm), rates of change are presented in millimeters (mm)

represented by a sum fixed basis function b_{jk}, multiplied by a coefficient β_{jk}, which needs to be estimated as

$$f_j(X_j) = \sum_{k=1}^{K} \beta_{jk} b_{jk}(x_j)$$

where K is the basis size and determines the maximum complexity of each smoother. The basis size represents the maximum possible degrees of freedom for each model term (Wood 2017).

The factor-smooth interaction without a global smooth term was included so that a different smooth would be generated for each station at a site, thereby allowing comparisons to be made between sites and refuges.

We used restricted maximum likelihood (REML) to estimate the smoothing parameters of the spline in each model. Specifically, we used the penalized regression smoothing method from the Mixed GAM Computation Vehicle (mgcv) R package (Wood 2000; Wood 2020; see Couvillion et al. 2017 for an application of this approach). Given the relatively low number of surface elevation and vertical accretion measurements for each site, each site-level GAM model was initially parameterized with a maximum basis size (K) of three to minimize over-fitting. To determine if the initial K value of three was adequate to represent any non-linear patterns in the data, function 'gam.check' from the 'mgcv' package was used to ensure that each model conformed to the model assumptions and to evaluate the K-index values for each level of the factor-smooth interaction between time and station. K-index values less than one can indicate that K may be too small to adequately capture the non-linear patterns (Wood 2017, 2020). When the K-index values for a model indicated that the initial K value of three was too

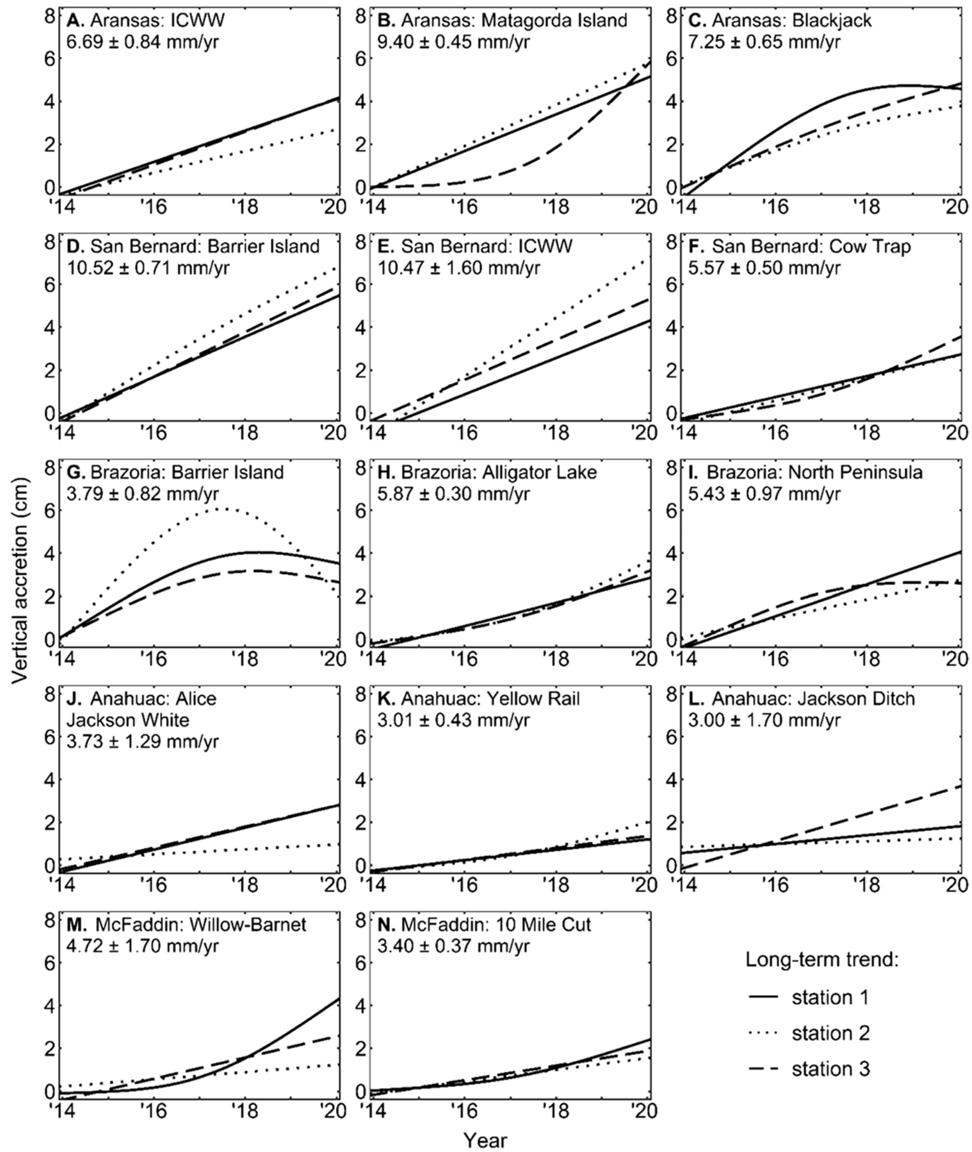

Fig. 3 Vertical accretion from marker horizons at the 14 coastal marsh sites. Generalized additive model-based results for each station at each site are presented in panels as black lines. Values in the plot labels represent the site-level rate of vertical accretion (mean ± standard error). Note that while vertical accretion on the y-axis is presented in centimeters (cm), rates of change are presented in millimeters (mm)

low for the factor-smooth interaction term, we increased K until the model fit had stabilized, up to a maximum K of five. The model was considered stabilized when subsequent increases to K did not affect the value of the model's smoothing parameter selection score or the effective degrees of freedom for the factor-smooth interaction term (Wood 2020).

To account for potential correlation among repeated observations from the same SET-MH station, we then plotted the autocorrelation function (ACF) and partial autocorrelation function (PACF) of the Pearson residuals of each site-level model against different lag periods to examine the presence of residual autocorrelation. If the ACF or PACF plots indicated the presence of residual autocorrelation for a particular site-level model, the model was updated using the 'gamm' function from the 'mgcv' package to include a 1.st order autocorrelation structure with a site-specific lag-1 autocorrelation value using the 'corAR1' function from the 'nlme' package (Pinheiro et al. 2021) with model form

$$g(\mu_t) = \beta_0 + \sum_{i=1}^{n} f_j(X_j) + \sum_{j=1}^{p} c_j\left(g(y_{t-j}) - \sum_{i=1}^{n} X_{t-j,i} f_j\right) + \varepsilon$$

where $\sum_{j=1}^{p} c_j\left(g(y_{t-j}) - \sum_{i=1}^{n} X_{t-j,i} f_j\right)$ are the autoregressive terms (AR1) that control the degree with which the random walk reverts to the mean as part of the AR time series.

The parameters for the site-level models of surface elevation change are shown in Table S3, whereas parameters for the site-level models of vertical accretion are shown in Table S4. Using the site-level fitted GAM models, we then calculated the rate of surface elevation change and vertical accretion at each station as the mean of 200 equally-spaced first derivatives of the function representing the factor-smooth interaction term in each model. The first derivatives of the factor-smooth interaction terms were estimated by finite-difference approximation via the 'derivatives' function from the R package 'gratia' (Simpson 2021; see Simpson 2018 for an application of this approach). Subsurface change at each station was calculated as the difference between elevation change (i.e., surface elevation change) and vertical accretion (Lynch et al. 2015; Cahoon et al. 2020). Station-level rates of elevation change, vertical accretion and subsurface change are provided in Table S1.

Data Analyses: Refuge and Site Comparisons

Linear mixed-effects models were used to compare rates of surface elevation change, vertical accretion, and subsurface change between refuges via the 'lmer' function from the R package 'lme4' (Bates et al. 2020). To account for correlation due to the nested nature of the sites within the refuges, we fit a simple linear-mixed effects model of the form

$$Y_i = \beta_0 + \beta_1 a_j + \varepsilon_{i(j)}$$

where Y_i represent the station-level rates of elevation change, vertical accretion, or subsurface change for the i^{th} station, $\beta's$ are fixed effects regression parameters with the refuge as a main effect, and $\varepsilon_{i(j)}$ is the random error associated with site i in refuge factor level j^i. For comparisons between sites, we used a linear model where the station-level rates of surface elevation change, vertical accretion, or subsurface change were the dependent variables and site was the independent variable. The R package 'lmerTest' was used to determine F and p values while correcting the denominator degrees of freedom using the Kenward-Rogers approximation (Kuznetsova et al. 2013). If there were significant differences between refuges or sites, post-hoc Tukey HSD tests were used to assess pairwise comparisons between refuges or between sites using the function 'cld' from the R package 'multcomp' (Torsten et al. 2021). Site-level rates were calculated as the average of the three station-level rates at each site, and refuge-level rates were calculated as the average of the site-level rates at each refuge.

Data Analyses: Hurricane Harvey Effects

We used a series of simple linear regressions to assess the effects of the distance from the landfall of Hurricane Harvey on sediment deposition and elevation dynamics, where the straight-line distance from the point of landfall to each site was the independent variable, and depth of the storm layer, rate of vertical accretion, and rate of elevation change at each site were the dependent variables. We also used a series of simple linear regressions to determine the influence of storm sediment deposits from Hurricane Harvey on rates of vertical accretion and elevation change, where the depth of the storm layer at each site was the independent variable, and the vertical accretion or elevation change rate at each site were the response variables. The site-level rates of elevation change and vertical accretion used in the linear regressions were derived from fitted GAM models as described in the previous section. All data analyses were conducted in R (R Core Team 2019) and maps were created in ArcGIS (Esri, Redlands, California, USA). Error terms throughout the manuscript are standard errors.

Results

Recent Sea-level Rise Rates

For Aransas NWR, the recent tidal epoch-based SLR rate (9.74 ± 1.78 mm yr^{-1}) was estimated from the Rockport gauge (ID: 8774770). For San Bernard and Brazoria NWRs, the recent tidal epoch-based SLR rate (6.81 ± 1.72 mm yr^{-1}) was estimated from the Freeport gauge (ID: 8772447). For Anahuac NWR, the recent tidal epoch-based SLR rate (11.68 ± 1.75 mm yr^{-1}) was estimated from the Galveston Pier-21 gauge (ID: 8771450). For McFaddin NWR, the recent tidal epoch-based SLR rate (11.36 ± 1.89 mm yr^{-1}) was estimated from the Sabine Pass gauge (ID: 8770570). The long-term historical relative sea-level rise rates from these tide gauges range from 4.21 to 6.55 mm/yr (NOAA 2020) as follows: Rockport gauge: 5.77 ± 0.49 mm yr^{-1} for 1937–2019; Freeport gauge: 4.21 ± 0.72 mm yr^{-1} for 1954–2020; Galveston Pier-21 gauge: 6.55 ± 1.22 mm yr^{-1} for 1904–2019; Sabine Pass gauge: 6.05 ± 0.74 mm yr^{-1} for 1958–2019.

Surface Elevation, Subsurface Elevation, and Vertical Accretion

Refuge-level comparisons are presented in Tables 2 and S5. Station-level surface elevation change data, analyses, and rates are shown in Tables S1 and S3 and Figs. 2 and S1-S3. There was a significant difference in surface elevation change between sites ($F_{13,28} = 9.54$, $p < 0.001$, $r^2 = 0.73$; Table 2; Fig. 2). Site-level rates of elevation change ranged from a low of -1.57 ± 0.69 mm yr^{-1} at Yellow Rail to a high of 8.37 ± 0.77 mm yr^{-1} at SB-Barrier Island (Table 2; Fig. 2). Station-level vertical accretion data, analyses, and rates are shown in Tables S1 and S4 and Figs. 3 and S4-S6. There was a significant difference in vertical accretion between sites ($F_{13,28} = 6.95$, $p < 0.001$, $r^2 = 0.65$; Table 2; Fig. 3). Site-level rates of vertical accretion ranged from a low of 3.00 ± 1.70 mm yr^{-1} at Jackson Ditch to a high of 10.52 ± 0.71 mm yr^{-1} at SB-Barrier Island (Table 2; Fig. 3). Station-level subsurface change rates are shown in Table S1. There was a significant difference in subsurface change

Table 2 Site- and refuge-level comparisons of rates of elevation change, vertical accretion, and subsurface change (mean ± SE). Within each column, site-level means with different lowercase letters are significantly different at $p < 0.05$. Within each column, refuge-level means with different uppercase letters are significantly different at $p < 0.05$

Refuge	Location	Elevation change (mm yr.$^{-1}$)	Vertical accretion (mm yr.$^{-1}$)	Subsurface change (mm yr.$^{-1}$)
Aransas	AR-ICWW (Site-level)	1.38 ± 1.92^{ab}	6.69 ± 0.84^{ac}	-5.31 ± 1.08^{ab}
	Matagorda Island (Site-level)	2.24 ± 0.76^{ab}	9.40 ± 0.45^{bc}	-7.16 ± 1.18^{a}
	Blackjack (Site-level)	1.13 ± 1.21^{ab}	7.25 ± 0.65^{ac}	-6.12 ± 1.79^{ab}
	Refuge-level	1.58 ± 0.71^{A}	7.78 ± 0.53^{AB}	-6.20 ± 0.70^{A}
San Bernard	SB-Barrier Island (Site-level)	8.37 ± 0.77^{c}	10.52 ± 0.71^{c}	-3.32 ± 1.03^{ab}
	SB-ICWW (Site-level)	7.86 ± 1.54^{c}	10.47 ± 1.60^{c}	-2.61 ± 2.69^{ab}
	Cow Trap (Site-level)	-0.38 ± 0.38^{a}	5.57 ± 0.50^{ac}	-5.95 ± 0.52^{ab}
	Refuge-level	5.29 ± 1.51^{A}	8.85 ± 0.98^{A}	-3.96 ± 0.99^{A}
Brazoria	BR-Barrier Island (Site-level)	5.26 ± 1.24^{bc}	3.79 ± 0.82^{a}	1.47 ± 1.61^{b}
	Alligator Lake (Site-level)	0.13 ± 0.14^{a}	5.87 ± 0.30^{ac}	-5.74 ± 0.41^{ab}
	North Peninsula (Site-level)	-0.44 ± 0.51^{a}	5.43 ± 0.97^{ac}	-5.87 ± 1.48^{ab}
	Refuge-level	1.65 ± 0.99^{A}	5.03 ± 0.49^{BC}	-3.38 ± 1.37^{A}
Anahuac	Alice Jackson White (Site-level)	1.24 ± 1.14^{ab}	3.73 ± 1.29^{a}	-2.49 ± 2.43^{ab}
	Yellow Rail (Site-level)	-1.57 ± 0.69^{a}	3.01 ± 0.43^{a}	-4.58 ± 0.40^{ab}
	Jackson Ditch (Site-level)	1.07 ± 0.48^{ab}	3.00 ± 1.70^{a}	-1.92 ± 2.17^{ab}
	Refuge-level	0.25 ± 0.61^{A}	3.25 ± 0.64^{C}	-3.00 ± 1.03^{A}
McFaddin	Willow-Barnet (Site-level)	0.93 ± 0.75^{ab}	4.72 ± 1.70^{ab}	-3.80 ± 1.71^{ab}
	10 Mile Cut (Site-level)	0.20 ± 0.63^{ab}	3.40 ± 0.37^{a}	-3.20 ± 0.82^{ab}
	Refuge-level	0.56 ± 0.47^{A}	4.06 ± 0.83^{BC}	-3.50 ± 0.86^{A}

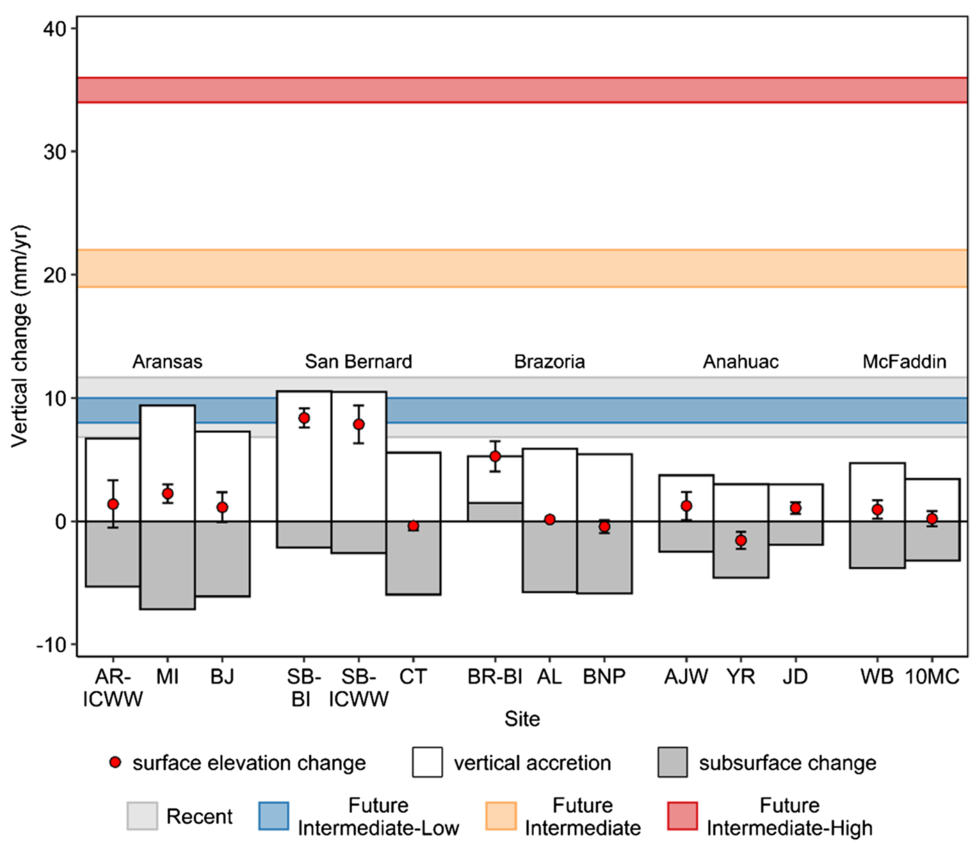

Fig. 4 Rates of surface elevation change, vertical accretion, and sub-surface elevation change at the 14 coastal marsh sites. Sub-surface elevation change represents the difference between surface elevation change and vertical accretion. Red points represent rates of surface elevation change (mean ± standard error). The gray area represents the range of recent local sea-level rise rates 2001–2019 from tide gauges on the Texas coast. The colored areas represent the range of estimated future local sea-level rise rates by 2100 for the Intermediate-Low (0.5 m; blue), Intermediate (1.0 m; orange), and Intermediate-High (1.5 m; red) global sea-level rise scenarios defined by Sweet et al. (2017). See Table 1 for definitions of site abbreviations

between sites ($F_{13,28} = 2.18$, $p < 0.05$, $r^2 = 0.27$; Table 2; Fig. 4). Site-level rates of subsurface change ranged from a low of -7.16 ± 1.18 mm yr^{-1} at Matagorda Island to a high of 1.47 ± 1.61 mm yr^{-1} at BR-Barrier Island (Table 2; Fig. 4).

Wetland Elevation Change in Relation to Recent and Future Sea-level Rise

Only two out of 14 sites had rates of elevation change greater than the recent rate of sea-level rise (Fig. 2). Two of the sites had a rate of elevation change close to the rate associated with the Intermediate-Low future sea-level rise scenario for the 2090–2100 decade (Fig. 4; see position of red circles relative to horizontal blue line). Under the Intermediate-Low sea-level rise scenario for the 2090–2100 decade, future projected local rates of relative sea-level rise are expected to be lowest for Anahuac and McFaddin NWRs (8 mm yr^{-1}), intermediate for Aransas NWR (9 mm yr^{-1}), and highest for San Bernard and Brazoria NWRs (10 mm yr^{-1}; Sweet et al. 2017). Under the Intermediate sea-level rise scenario, future projected local rates of relative sea-level rise for the 2090–2100 decade are expected to be lowest for Anahuac and McFaddin NWRs (19 mm yr^{-1}), intermediate for Aransas NWR (21 mm yr^{-1}), and the highest for San Bernard and Brazoria NWRs (22 mm yr^{-1}; Sweet et al. 2017). No sites had a rate of elevation change above the rates associated with the future Intermediate and Intermediate-High scenarios for the 2090–2100 decade. Under the Intermediate-High sea-level rise scenario, future projected local rates of sea-level rise for the 2090–2100 decade are expected to be lowest for Aransas NWR (34 mm yr^{-1}), intermediate for Anahuac and McFaddin NWRs (35 mm yr^{-1}), and highest for San Bernard and Brazoria NWRs (36 mm yr^{-1}; Sweet et al. 2017).

Hurricane Harvey Effects

Storm sediment deposits from Hurricane Harvey were observed at 10 of the 14 sites and ranged from a station-level high of 32.67 mm to a station-level low of 0.66 mm (Table S1). Storm deposits were highest at sites within San Bernard, Aransas, and Brazoria NWRs (Table S1), which are the sites closest to the landfall of Hurricane Harvey. There was a significant negative linear relationship between distance from the landfall of Hurricane Harvey and storm deposit depth ($F_{1,12} = 5.49$, $r^2 = 0.26$, $p < 0.05$; Fig. 5A). There was also a significant negative linear relationship between distance from the landfall of Hurricane Harvey and vertical accretion rates across the 2014–2019 study period ($F_{1,12} = 10.28$, $r^2 = 0.42$, $p < 0.01$; Fig. 5B). There was no relationship between the distance from the landfall of Hurricane Harvey and rates of elevation change across the 2014–2019 study period ($F_{1,12} = 0.72$, $p = $ ns; not graphed). However, there were significant, positive linear relationships between the depth of the storm deposit from Hurricane Harvey and rates of both vertical accretion ($F_{1,12} = 12.03$, $r^2 = 0.46$, $p < 0.01$; Fig. 6A) and elevation

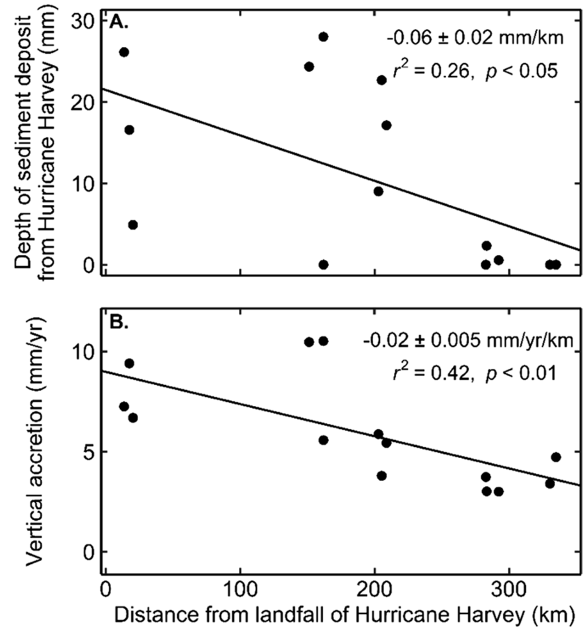

Fig. 5 The relationships between the distance from the Hurricane Harvey landfall and: (**A**) the depth of the deposit of suspended sediments from Hurricane Harvey, and (**B**) the rate of vertical accretion

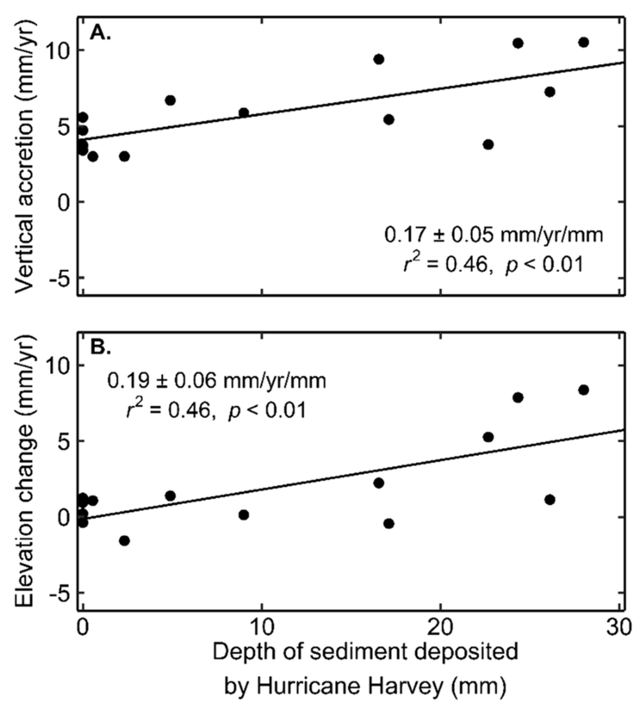

Fig. 6 The relationships between the depth of the deposit of suspended sediments from Hurricane Harvey and: (**A**) the rate of vertical accretion, or (**B**) the rate of elevation change

change ($F_{1,12}=12.11$, $r^2=0.46$ $p<0.01$; Fig. 6B) across the 2014–2019 study period.

Discussion

We examined surface elevation dynamics in five U.S. Fish and Wildlife Service National Wildlife Refuges that collectively span over half of the Texas coast. As public lands, these refuges are managed specifically to provide sustainable habitats for fish and wildlife. Our results indicate that these lands may be in jeopardy of loss or degradation because net elevation gains during our study period were often lower than recent relative sea-level rise rates and much lower than rates expected under future sea-level rise scenarios. These results raise substantial concern for the future of coastal marshes in Texas. The long-term ramifications of coastal marsh loss will be damaging not only to fish and wildlife, but also to local and regional economies and the nearly seven million Texans who live and work along the coast. Our results also demonstrate the significance of infrequent pulsing events – such as hurricanes – to the long-term resilience of these coastal wetlands. In the subsequent sections, we discuss coastal marsh surface elevation change dynamics and examine the implications for marsh stability in the face of rising seas and intensifying hurricanes.

How Do Rates of Coastal Marsh Surface Elevation Change, Vertical Accretion, and Subsurface Change Vary in Texas Coastal Marshes?

Across the Texas coast, there is variation in factors that affect surface elevation dynamics in coastal marshes (Longley 1994; Sweet et al. 2017; Osland et al. 2018). For example, gradients in geomorphology, landscape position, subsidence, relative sea-level rise, climate, salinity, and freshwater inflow affect inundation, plant growth, and sedimentation rates. In our study area, we documented large site-level differences in rates of surface elevation change, vertical accretion, and subsurface change (Figs. 2 and 3). For example, while the mean rate of surface elevation change was 1.96 ± 0.87 mm yr^{-1}, the range in site-level rates ranged from -1.57 to 8.37 mm yr^{-1} (Table 2). Vertical accretion gains were largest in sediment-rich, high-energy zones near Hurricane Harvey landfall.

The number and spatial extent of SET-MH stations included in this study (i.e., 42 stations, 14 sites) builds foundational knowledge of surface elevation dynamics in Texas coastal marshes. Prior to this communication, only a handful studies had incorporated SET-MH data from Texas (i.e., Cahoon et al. 2004; Cahoon et al. 2011; McKee and Grace 2012, Cressman 2020, Swanson 2020; see also regional SET-MH inventory in Osland et al. 2017). Advancing understanding of the variation in wetland surface elevation dynamics across this region will require a larger network of sites spanning the entire state, including gradients in geomorphology, landscape position, subsidence, relative sea-level rise, climate, salinity, vegetation composition, and freshwater inflow. For comparison, the Louisiana Coastwide Reference Monitoring System, which is the largest SET-MH network in the world, contains 332 SET-MH stations across an area roughly 1.6 times the size of our study area. Moreover, many other SET-MH stations in Louisiana are managed by research groups outside of the CRMS (Coastal Reference Monitoring System) network. The number of SET-MH stations in Louisiana outnumbers those in Texas by at least 5:1. One weakness of the SET-MH approach is the small spatial scale (i.e., several meters) that it directly represents. Thus, the SET-MH approach can be combined with complementary approaches that measure surface elevation change at larger spatial scales and higher spatial resolutions (e.g., Cain and Hensel 2018; Kargar et al. 2021).

At global and national scales, the majority of SET-MH studies have been conducted in graminoid-dominated salt marshes and mangrove forests (Webb et al. 2013; Osland et al. 2017). Fewer SET-MH studies have been conducted in succulent plant-dominated salt marshes or unvegetated salt flats (i.e., salt pannes, salt pans, salt barrens, sabkhas, salinas), which are coastal wetland ecosystems that are more common through the hypersaline conditions produced in arid and semi-arid climates (Zedler 1982; Ridd et al. 1988; Dunton et al. 2001; Withers 2002). Thus, this study fills an important gap in the literature as it contains surface elevation data from seven marsh sites that are dominated by succulent plants (Table 2). Soil organic matter development greatly influences wetland ecosystem structure, function, and stability via effects on surface elevation dynamics (Morris et al. 2002; Kirwan and Megonigal 2013). Along the Texas coast, soil organic matter development in coastal wetlands varies greatly and is strongly influenced by the combined effects of precipitation, freshwater inputs, salinity, and plant productivity (Osland et al. 2018). As a result, coastal Texas is an outstanding natural laboratory for investigating the effects of changing precipitation, freshwater inflow, and salinity regimes on coastal ecosystems (e.g., Longley 1994, 1995; Dunton et al. 2001; Alexander and Dunton 2002; Forbes and Dunton 2006; Montagna et al. 2007; Osland et al. 2014, 2016, 2018, 2019; Gabler et al. 2017). Soil organic matter development is typically lower in salt flats and succulent plant-dominated salt marshes (Osland et al. 2018). While this study begins to advance our understanding of the effects of succulent plants on surface elevation change dynamics, our study design was not developed to explicitly examine the effects of gradients in rainfall, salinity, plant productivity, and plant functional group dominance. Thus, there is still a need for studies that examine surface elevation dynamics across these gradients and especially in the salt flats and succulent plant-dominated wetlands that are abundant along the southern and central Texas coast (i.e., within the Lower Laguna Madre, Upper Laguna Madre, Nueces, Mission-Aransas, Guadalupe, and Colorado-Lavaca estuaries).

What was the Effect of Hurricane Harvey Sediments on Vertical Accretion and Surface Elevation Change in Coastal Marshes?

Hurricane sediments can build elevation and increase elevation capital (Cahoon et al. 2019), enabling coastal wetlands to better keep pace with sea-level rise (McKee and Cherry 2009; Baustian and Mendelssohn 2015; Feher et al. 2020; Osland et al. 2020). However, storm-derived sediment deposition in coastal marsh habitats is highly variable and dependent upon storm intensity, landscape position, tidal nexus, and sediment size (Du et al. 2019; Williams and Liu 2019; Yao et al. 2020; Kuhn et al. 2021). Williams (2010) studied storm deposition from Hurricane Ike (2008) on McFaddin National Wildlife Refuge and documented fine storm sediments as far as 2.7 km inland from marine habitats and found that the storm deposited a layer of sediment approximately 10 cm thick in Clam Lake, a large brackish wetland approximately 2 km inland. Williams and Denlinger (2013) estimated an average of 30 cm of sedimentation from Hurricane Ike along a transect between Clam Lake and the beach on McFaddin National Wildlife Refuge. This constitutes roughly 54% of the sediment deposition between 1950 to 2008, indicating that storm deposition can be a major factor driving accretion rates in this region (Williams and Denlinger 2013).

In an analysis of surface elevation trends along the Atlantic coast of the United States following Hurricane Sandy, Cahoon et al. (2019) and Yeates et al. (2020) used data from a network of SET-MH sites to show that landscape position relative to hurricane landfall greatly influences wetland surface elevation dynamics. Our study reinforces this conclusion. Within our study period, Hurricane Harvey provided the most prolific and measurable effect on surface elevation change dynamics at our study sites. During this event, many of our study sites received substantial sediment inputs due to a combination of storm surge and/or freshwater flooding from high levels of storm-produced rainfall (Du et al. 2019; Williams and Liu 2019; Yao et al. 2020; Kuhn et al. 2021). In general, sediment deposition was highest in some sites located close to Hurricane Harvey's landfall; however, there was much variation in sedimentation near landfall, indicating that landscape position and other factors influence spatial patterns of sediment deposition within wetlands close to hurricane landfall (Fig. 5A, B). Conversely, our sites that were far from landfall had consistently lower sedimentation rates. We also identified positive relationships between the Harvey sediment depth and rates of vertical accretion and surface elevation change (Fig. 6A, B).

Despite the accretion events linked to tropical storm and hurricane events, post-hurricane elevation losses can ensue due to erosion, storm sediment compaction, and/or root zone compaction (McKee and Cherry 2009). We documented storm sediment compaction or erosion at some stations in Aransas and Brazoria National Wildlife Refuges (Figs. S4 and S5). Compaction or erosion at the BR-Barrier Island site was most pronounced with approximately 1.5 mm of change occurring over a 2-year period post Hurricane Harvey. While we did not measure root zone compaction, the lack of biogenic accretion at the majority of our study sites indicates that the root zone is not expanding in most locations. Based upon our results and those from other parts of the Gulf of Mexico (e.g., Baumann et al. 1984; DeLaune et al. 1983; Baustian et al. 2012; Cahoon and Reed 1995; Cahoon et al. 1995a, b; Reed 2002; McKee and Cherry 2009; Feher et al. 2020; Yao et al. 2020; Castañeda-Moya et al. 2020; McKee et al. 2020), we expect storm events to continue to be important drivers of surface elevation change dynamics in coastal wetlands along the Texas coast.

How Do Rates of Surface Elevation Change in Coastal Marshes Compare with Historical, Recent, and Expected Future Rates of Relative Sea-level Rise?

Positive feedbacks between inundation, plant growth, and sedimentation can enable some wetlands to adjust to moderate rates of sea-level rise (Gough and Grace 1998; Cahoon 2006; Nyman et al. 2006; Stagg et al. 2020). However, there are limits to coastal wetlands' ability to build sufficient elevation to adapt to rising seas (Saintilan et al. 2020; Törnqvist et al. 2020). There are several factors that make coastal wetlands in Texas particularly vulnerable to sea-level rise. These include comparatively high rates of subsidence and relative sea-level rise (Sweet et al. 2017), small tidal ranges (Kirwan et al. 2016), and anthropogenic land-use changes that have reduced freshwater and sediment delivery to the coast (Longley 1994).

Marsh surface elevation gains at our sites were often lower than long-term historical relative sea-level rise rates (NOAA 2020), local recent relative sea-level rise rates (Fig. 2), and much smaller than accelerated sea-level rise rates expected by the end of the twenty-first century (Sweet et al. 2017; Fig. 4). The differences between rates available for marsh surface elevation change in comparison with sea-level rise further reinforce that site selection, marsh type, and dominant vegetation are likely factors that warrant careful consideration for development of future monitoring efforts. Because our study indicates wetlands in our study area are not keeping pace with recent sea-level rise rates, it is unlikely that they will be able to build elevation to keep pace with future predicted accelerations in sea-level rise. While tipping points for marsh conversion to open water are variable, accelerated relative sea-level rise rates predicted within our study area make wetland conversion to open water likely within the twenty-first century (Paine 1993; Coplin and Galloway 1999; Morton et al. 2006; Ramage and Shah 2019; Stagg et al. 2020; Törnqvist 2020). Marsh drowning could affect the many ecosystem services and societal benefits provided by coastal wetlands, including storm surge protection, buffering flood damages, erosion regulation, fisheries production, carbon sequestration, and water quality improvements (Nicholls and Leatherman 1995; Engle 2011; Jadhav et al. 2013; Mendelssohn et al. 2017). Loss of coastal wetlands to sea-level rise could have far-reaching implications to the nearly seven million Texans living adjacent to the coastline (Texas Comptroller Office 2020).

The rates of elevation change measured in this study are low relative to recent sea-level rise rates, indicating that coastal wetland fragmentation and loss are possible in this region. In Louisiana, spatial and temporal patterns of coastal wetland loss are periodically measured at the state level (e.g., Couvillion et al. 2017), which provides valuable information for coastal restoration planning efforts. Our results, along with the findings from other studies conducted in Texas (e.g., Moulton et al. 1997; Armitage et al. 2015; Entwistle et al. 2018; Stagg et al. 2020) indicate that state-level analyses of wetland loss could inform resource management decisions in Texas. Given the high rates of recent relative sea-level rise and the low rates of surface elevation change in coastal marshes, there is a need to better measure spatial and temporal patterns of coastal wetland fragmentation and loss in Texas.

Minimizing Wetland Loss in Texas

Our data highlight the importance of restoration, conservation actions in coastal marshlands along Texas' Gulf of Mexico coast. Given the potential for coastal wetland fragmentation and loss, proactive planning for mitigation of impacts of various scenarios of predicted sea-level rise may inform future resource management actions. Ecosystem restoration can improve the structure, function, and stability of coastal marshes in the face of rising sea-levels and intensifying hurricanes. Strategies for building elevation capital and enhancing surface elevation change include: (1) beneficial use of dredged material to increase marsh elevation and decrease erosion (Turner and Streever 2002; Ganju 2019); (2) providing conditions that maximize the productivity of marsh foundation plants that can foster positive biogenic feedbacks (Boesch et al. 1994; Turner and Streever 2002); (3) strategic placement of breakwaters, ridges, or marsh terraces in high-energy environments to reduce erosion (Steyer 1993; Boesch et al. 1994; Turner and Streever 2002; Brasher 2015; Osorio et al. 2020); and (4) restoration of tidal connectivity and freshwater inflows to improve abiotic conditions (Boesch et al. 1994; Turner and Streever 2002; Natural Resource Council 2014). For some coastal wetlands, where fire has historically played an important role in shaping coastal landscapes, there is a need to investigate the influence of managed fires on marsh plant productivity, wetland fragmentation, and surface elevation dynamics (Cahoon et al. 2004; McKee and Grace 2012; Braswell et al. 2019). Marsh restoration and management actions can enhance marsh resilience, reduce wetland loss, and improve plant community productivity and composition (Chabreck 1989; Nyman et al. 1993; Boesch et al. 1994; DeLaune et al. 1994; Nyman and Chabreck 2012; Natural Resource Council 2014). Methods that increase elevation and/or accelerate biogeomorphic processes can improve marsh stability in the face of accelerated sea-level rise and intensifying hurricanes. Where local marsh loss is expected in response to high rates of relative sea-level rise, development of landscape adaptation plans that proactively facilitate the landward migration of coastal marshes into adjacent upslope and upriver ecosystems can be used to partially mitigate for seaward wetland losses. Due to the low-lying coastal topography in this region, there is some room for tidal saline wetlands to move landward into adjacent freshwater wetland and upland ecosystems (Enwright et al. 2016; Borchert et al. 2018).

Supplementary Information The online version contains supplementary material available at https://doi.org/10.1007/s13157-022-01565-3.

Acknowledgements We thank Larry Allain, Jeremy Edwardson, Sue Wilder, Dr. Grant Harris, Thomas Adams, Roland Davis, Stephen LeJeune, Bryan Carethers, Ronald DeRoche, Jim Steinbaugh, Andrew Stetter, Colt Sanspree, Maxwell Boyle, Stephanie Goehring, Amanda Chesnutt, Nancy Brown, Caitlyn Wade, Julia Scruggs, Stacey Kinney, Meghan Maurin, Douglas Head I, and Dena McNeil for assistance with either installing surface elevation table study sites or assisting with data collection. We also thank USFWS staff from the Texas Chenier Plain, Texas Mid-Coast NWR Complexes and Aransas NWR for providing logistical and field support for the project. This work was made possible by the financial support of USFWS NWR System. This work was supported in part by the U.S. Geological Survey (USGS) Ecosystems, Climate R&D, and Greater Everglades Priority Ecosystem Science Programs. We appreciate the swift and thorough review of our manuscript by Grant Harris and Scott Jones. The findings and conclusions in this article are those of the author(s) and do not necessarily represent the views of the U.S. Fish and Wildlife Service. Any use of trade, firm, or product names is for descriptive purposes only and does not imply endorsement by the U.S. Government. Texas National Wildlife Refuge sediment elevation and marker horizon data generated in this study are available as a U.S. Fish and Wildlife Service data release (Moon et al. 2021) at https://doi.org/10.7944/P9CBFO1C.

Author Contribution Jena A. Moon, William C. Vervaeke, Douglas M. Head, Kristine L. Metzger, and Nicole M. Rankin conceived and designed the study. Jena A. Moon, Tiffany C. Lane, William C.

Vervaeke, Douglas M. Head, Laura C. Feher, and Bogdan C. Chivoiu collected data. Jena A. Moon, Laura C. Feher, Tiffany C. Lane, William C. Vervaeke, Douglas M. Head, and Bogdan C. Chivoiu organized and prepared data for analyses. Laura C. Feher conducted data analyses with feedback from Michael J. Osland, Jena A. Moon, William C. Vervaeke, David R. Stewart, Darren J. Johnson, and James B. Grace. Jena A. Moon, Michael J. Osland, Laura C. Feher, Tiffany C. Lane, William C. Vervaeke wrote the first manuscript draft. All authors provided comments on subsequent drafts. All authors read and approved the final manuscript.

Funding This work was made possible by the financial support of USFWS NWR System. This work was also supported in part by the USGS Ecosystems, Climate R&D, and Greater Everglades Priority Ecosystem Science Programs.

Data Availability Texas National Wildlife Refuge sediment elevation and marker horizon data generated in this study are available at https://doi.org/10.7944/P9CBFO1C (Moon et al. 2021).

Code Availability N/A.

Declarations

Ethics Approval N/A.

Consent to Participate N/A.

Consent for Publication Yes.

Conflicts of Interest/Competing Interests No conflict of interest or competing interest to report.

References

Alexander HD, Dunton KH (2002) Freshwater inundation effects on emergent vegetation of a hypersaline salt marsh. Estuaries and Coasts 25:1426–1435

Armitage AR, Highfield WE, Brody SD, Louchouarn P (2015) The contribution of mangrove expansion to salt marsh loss on the Texas Gulf Coast. PLoS ONE 10:e0125404

Barbier EB, Hacker SD, Kennedy C, Koch EW, Stier AC, Silliman BR (2011) The value of estuarine and coastal ecosystem services. Ecological Monographs 81:169–193

Bates D, Mächler MM, Bolker BM, Walker SC (2020) lme4: Linear mixed-effects models using 'Eigen' and S4. R package version 1.1–26. http://CRAN.R-project.org/package=lme4

Baumann RH, Day JW Jr, Miller CA (1984) Mississippi deltaic wetland survival: Sedimentation versus coastal submergence. Science 224:1093–1095

Baustian JJ, Mendelssohn IA (2015) Hurricane-induced sedimentation improves marsh resilience and vegetation vigor under high rates of relative sea-level rise. Wetlands 35:795–802

Baustian JJ, Mendelssohn IA, Hester MW (2012) Vegetation's importance in regulating surface elevation in a coastal salt marsh facing elevated rates of sea-level rise. Global Change Biology 18:3377–3382

Blake ES, Zelinsky DA (2018) Tropical Cyclone Report, Hurricane Harvey (AL092017). National Weather Service, National Hurricane Center, Miami, FL

Blum M, Roberts HH (2009) Drowning of the Mississippi Delta due to insufficient sediment supply and global sea-level rise. Nature Geoscience 2:488–491

Boesch, DF, Josselyn MN, Mehta AJ, Morris JT, Nuttle WK, Simestad CA, Swift DJP (1994) Scientific assessment of coastal wetland loss, restoration and management in Louisiana. Journal of Coastal Research, Special Issue No. 20. Scientific Assessment of Coastal Wetland Loss, Restoration and Management in Louisiana:1–103

Borchert SM, Osland MJ, Enwright NM, Griffith KT (2018) Coastal wetland adaptation to sea-level rise: quantifying potential for landward migration and coastal squeeze. Journal of Applied Ecology 55:2876–2887

Brasher MG (2015) Review of the benefits of marsh terraces in the northern Gulf of Mexico. Ducks Unlimited, Inc., Gulf Coast Joint Venture, Lafayette, LA

Braswell AE, May CA, Cherry JA (2019) Spatially-dependent patterns of plant recovery and sediment accretion following multiple disturbances in a Gulf Coast tidal marsh. Wetlands Ecology and Management 27:377–392

Cahoon DR (2006) A review of major storm impacts on coastal wetland elevations. Estuaries and Coasts 29:889–898

Cahoon DR, Reed DJ (1995) Relationships among marsh surface topography, hydroperiod, and soil accretion in a deteriorating Louisiana salt marsh. Journal of Coastal Research 11:357–369

Cahoon DR, Turner RE (1989) Accretion and canal impacts in a rapidly subsiding wetland. II. Feldspar marker horizon technique. Estuaries 12:260–268

Cahoon DR, Reed DJ, Day JW Jr (1995a) Estimating shallow subsidence in microtidal salt marshes of the southeastern United States: Kaye and Barghoorn revisited. Marine Geology 128:1–9

Cahoon DR, Lynch JC, Hensel P, Boumans R, Perez BC, Segura B, Day JW Jr (2002a) High-precision measurements of wetland sediment elevation: I. Recent improvements to the sedimentation-erosion table. Journal of Sedimentary Research 72:730–733

Cahoon DR, Lynch JC, Perez BC, Segura B, Holland RD, Stelly C, Stephenson G, Hensel P (2002b) High-precision measurements of wetland sediment elevation: II. The rod surface elevation table. Journal of Sedimentary Research 72:734–739

Cahoon DR, Hensel P, Rybczyk J, McKee KL, Proffitt CE, Perez BC (2003) Mass tree mortality leads to mangrove peat collapse at Bay Islands, Honduras after Hurricane Mitch. Journal of Ecology 91:1093–1105

Cahoon DR, Ford MA, Hensel PF (2004) Ecogeomorphology of *Spartina patens* dominated tidal marshes: soil organic matter accumulation, marsh elevation dynamics, and disturbance. In: Fagherazzi S, Marani M, Blum LK (eds) The ecogeomorphology of tidal marshes. American Geophysical Union, Washington, DC, pp 247–266

Cahoon DR, Perez BC, Segura BD, Lynch JC (2011) Elevation trends and shrink–swell response of wetland soils to flooding and drying. Estuarine, Coastal and Shelf Science 91:463–474

Cahoon DR, Lynch JC, Roman CT, Schmit JP, Skidds DE (2019) Evaluating the relationship among wetland vertical development, elevation capital, sea-level rise, and tidal marsh sustainability. Estuaries and Coasts 42:1–15

Cahoon DR, Reed DJ, Day JW, Lynch JC, Swales A, Lane RR (2020) Applications and utility of the surface elevation table–marker horizon method for measuring wetland elevation and shallow soil subsidence-expansion. Geo-Marine Letters 40:809–815

Cahoon, DR, Reed DJ, Day JW, Steyer GD, Boumans RM, Lynch JC, McNally D, Latif N (1995b) The influence of Hurricane Andrew on sediment distribution in Louisiana coastal marshes. Journal of Coastal Research, Special Issue No 21. Impacts of Hurricane Andrew on the Coastal Zones of Florida and Louisiana: 280–294

Cain MR, Hensel PF (2018) Wetland elevations at sub-centimeter precision: exploring the use of digital barcode leveling for elevation monitoring. Estuaries and Coasts 41:582–591

Callaway JC, Cahoon DR, Lynch JC (2013) The surface elevation table–marker horizon method for measuring wetland accretion and elevation dynamics. In: DeLaune RD, Reddy KR, Richardson CJ, Megonigal JP (eds) Methods in Biogeochemistry of Wetlands. Soil Science Society of America, Madison, WI, pp 901–917

Castañeda-Moya E, Rivera-Monroy VH, Chambers RM, Zhao X, Lamb-Wotton L, Gorsky A, Gaiser EE, Troxler TG, Kominoski JS, Hiatt M (2020) Hurricanes fertilize mangrove forests in the Gulf of Mexico (Florida Everglades, USA). PNAS 9:4831–4841

Chabreck RH (1989) Creation, restoration and enhancement of north central Gulf coast marshes. In: Kusler JA, Kentula ME (eds) Wetland creation and restoration: the status of the science, vol I. Regional reviews, EPA/600/3–89/038a. Environmental Protection Agency, Research Laboratory, Corvallis, OR

Coplin LS, Galloway D (1999) Houston-Galveston, Texas—Managing coastal subsidence. In: Galloway D, Jones DR, Ingebritsen SE (eds) Land subsidence in the United States, USGS Circular 1182. U.S. Geological Survey, Reston, VA, pp 35–48

Costanza R, de Groot R, Sutton P, van der Ploeg S, Anderson SJ, Kubiszewski I, Farber S, Turner RK (2014) Changes in the global value of ecosystem services. Global Environmental Change 26:152–158

Couvillion BR, Beck H, Schoolmaster D, Fischer M (2017) Land area change in coastal Louisiana (1932 to 2016): U.S. Geological Survey Scientific Investigations Map 3381. https://doi.org/10.3133/sim3381

Cressman K (2020) National Synthesis of NERR SET Data. Grand Bay National Estuarine Research Reserve, MS. https://nerrssciencecollaborative.org/resource/national-synthesis-nerr-surface-elevation-table-data. Accessed 9 Mar 2022

Daily GC, Matson PA, Vitousek PM (1997) Ecosystem services supplied by soil. In: Daily GC (ed) Nature's services: Societal dependence on natural ecosystems. Island Press, Washington, DC, pp 113–132

Day JW Jr, Britsch LD, Hawes SR, Shaffer GP, Reed DJ, Cahoon DR (2000) Pattern and process of land loss in the Mississippi Delta: A spatial and temporal analysis of wetland habitat change. Estuaries 23:425–438

DeLaune RD, Baumann RH, Gosselink JG (1983) Relationships among vertical accretion, coastal submergence, and erosion in a Louisiana Gulf Coast marsh. Journal of Sedimentary Petrology 53:147–157

DeLaune RD, Nyman JA, Patrick WH Jr (1994) Peat collapse, ponding and wetland loss in a rapidly submerging coastal marsh. Journal of Coastal Research 10:1021–1030

Du J, Park K, Dellapenna TM, Clay JM (2019) Dramatic hydrodynamic and sedimentary responses in Galveston Bay and adjacent inner shelf to Hurricane Harvey. Science of the Total Environment 653:554–564

Dunton KH, Hardegree B, Whitledge TE (2001) Response of estuarine marsh vegetation to interannual variations in precipitation. Estuaries and Coasts 24:851–861

Engle VD (2011) Estimating the provision of ecosystem services by Gulf of Mexico coastal wetlands. Wetlands 31:179–193

Entwistle C, Mora MA, Knight R (2018) Estimating coastal wetland gain and losses in Galveston County and Cameron County, Texas, USA. Integrated Environmental Assessment and Management 14:120–129

Enwright NM, Griffith KT, Osland MJ (2016) Barriers to and opportunities for landward migration of coastal wetlands with sea-level rise. Frontiers in Ecology and the Environment 14:307–316

Enwright NM, Hartley SB, Couvillion BR, Brasher MG, Visser JM, Mitchell MK, Ballard BM, Parr MW, Wilson BC (2015) Delineation of marsh types from Corpus Christi Bay, Texas, to Perdido Bay, Alabama, in 2010: U.S. Geological Survey Scientific Investigations Map 3336. https://doi.org/10.3133/sim3336

ESRI (2020) ArcGIS Desktop: Release 10. Environmental Systems Research Institute, Redlands, CA

Feher LC, Osland MJ, Anderson GH, Vervaeke WC, Krauss KW, Whelan KRT, Balentine KM, Tiling-Range G, Smith TJ III, Cahoon DR (2020) The long-term effects of hurricanes Wilma and Irma on soil elevation change in everglades mangrove forests. Ecosystems 23:917–931

Forbes MG, Dunton KH (2006) Response of a subtropical estuarine marsh to local climatic change in the southwestern Gulf of Mexico. Estuaries and Coasts 29:1242–1254

Gabler CA, Osland MJ, Grace JB, Stagg CL, Day RH, Hartley SB, Enwright NM, From AS, McCoy ML, McLeod JL (2017) Macroclimatic change expected to transform coastal wetland ecosystems this century. Nature Climate Change 7:142–147

Ganju NK (2019) Marshes are the new beaches: Integrating sediment transport into restoration planning. Estuaries and Coasts 42:917–926

Gillins DT, Kerr D, Weaver B (2019) Evaluation of the online positioning user service for processing static GPS surveys: OPUS-Projects, OPUS-S, OPUS-Net, and OPUS-RS. ASCE Journal of Surveying Engineering 145:05019002

Gough L, Grace JB (1998) Herbivore effects on plant species density at varying productivity levels. Ecology 79:1586–1594

Jadhav RS, Chen Q, Smith JM (2013) Spectral distribution of wave energy dissipation by salt marsh vegetation. Coastal Engineering 77:99–107

Kargar AR, MacKenzie RA, Fafard A, Krauss KW, van Aardt J (2021) Surface elevation change evaluation in mangrove forests using a low-cost, rapid-scan terrestrial laser scanner. Limnology and Oceanography: Methods 19:8–20

Kirwan ML, Megonigal JP (2013) Tidal wetland stability in the face of human impacts and sea-level rise. Nature 504:53–60

Kirwan M, Temmerman S, Skeehan E, Guntenspergen G, Fagherazzi S (2016) Overestimation of marsh vulnerability to sea level rise. Nature Clim Change 6:253–260. https://doi.org/10.1038/nclimate2909

Kossin JP, Hall T, Knutson T, Kunkel KE, Trapp RJ, Waliser DE, Wehner MF (2017) Extreme storms. In: Wuebbles DJ, Fahey DW, Hibbard KA, Dokken DJ, Stewart BC, Maycock TK (eds) Climate Science Special Report: Fourth National Climate Assessment, Volume I. U.S. Global Change Research Program, Washington, DC, pp 257–276

Krauss KW, Osland MJ (2020) Tropical cyclones and the organization of mangrove forests: A review. Annals of Botany 125:213–234

Kuhn AL, Kominoski JS, Armitage AR, Charles SP, Pennings SC, Weaver CA, Maddox TR (2021) Buried hurricane legacies: increased nutrient limitation and decreased root biomass in coastal wetlands. Ecosphere 12:e03674

Kuznetsova A, Brockhoff PB, Christensen RHB (2013) lmerTest: Tests for random and fixed effects for linear mixed models (lmer objects of lme4 package). R package version 2.0–0. http://CRAN.R-project.org/package=lmerTest

Longley WL (1994) Freshwater inflows to Texas bays and estuaries: Ecological relationships and methods for determination of needs. Texas Water Development Board and Texas Parks and Wildlife Department, Austin, TX

Longley WL (1995) Estuaries. In: North GR, Schmandt J, Clarkson J (eds) The impact of global warming on Texas: A report to the task force on climate change in Texas. The University of Texas, Austin, TX, pp 88–118

Lynch JC, Hensel P, Cahoon DR (2015) The surface elevation table and marker horizon technique: A protocol for monitoring wetland elevation dynamics, Natural Resource Report NPS/NCBN/NRR—2015/1078. National Park Service, Fort Collins, CO

McKee KL, Cherry JA (2009) Hurricane Katrina sediment slowed elevation loss in subsiding brackish marshes of the Mississippi River delta. Wetlands 29:2–15
McKee KL, Grace JB (2012) Effects of prescribed burning on marsh-elevation change and the risk of wetland loss, U.S. Geological Survey Open-File Report 2012-1031. U.S. Geological Survey, Lafayette, LA
McKee K, Vervaeke WR (2018) Will fluctuations in salt marsh - mangrove dominance alter vulnerability of a subtropical wetland to sea-level rise? Glob Chang Biol 24. https://doi.org/10.1111/gcb.13945
McKee KL, Mendelssohn IA, Hester MW (2020) Hurricane sedimentation in a subtropical salt marsh-mangrove community is unaffected by vegetation type. Estuarine, Coastal and Shelf Science 239:106733
Mendelssohn IA, Byrnes MR, Kneib RT, Vittor BA (2017) Coastal habitats of the Gulf of Mexico. In: Ward C (ed) Habitat and biota of the Gulf of Mexico: Before the Deepwater Horizon oil spill. Springer, New York, New York, USA, pp 359–640
Montagna PA, Gibeaut JC, Tunnell JW Jr (2007) South Texas climate 2100: coastal impacts. In: Norwine J, John K (eds) The Changing Climate of South Texas 1900–2100: Problems and Prospects, Impacts and Implications. CREST-RESSACA. Texas A & M University, Kingsville, Texas, USA, pp 57–77
Moon JA, Feher LC, Lane TC, Vervaeke WC, Osland MJ, Head DM, Chivoiu BC (2021) Surface elevation change dynamics in coastal marshes along the northwestern Gulf of Mexico: building knowledge to better anticipate effects of rising sea-level and intensifying hurricanes: U.S. Fish and Wildlife Service data release. https://doi.org/10.7944/P9CBFO1C
Morris JT, Sundareshwar PV, Nietch CT, Kjerfve B, Cahoon DR (2002) Responses of coastal wetlands to rising sea level. Ecology 83:2869–2877
Morton RA, Bernier JC, Barras JA (2006) Evidence of regional subsidence and associated interior wetland loss induced by hydrocarbon production, Gulf Coast region, USA. Environmental Geology 50:261–274
Moulton DW, Dahl TE, Dall DM (1997) Texas coastal wetlands: status and trends, mid-1950s to early 1990s. U.S. Department of Interior, Fish and Wildlife Service, Albuquerque, NM
National Oceanic and Atmospheric Administration (2019a) Tides and Water Levels. https://oceanservice.noaa.gov/. Accessed 7 Mar 2021
National Oceanic and Atmospheric Administration (2019b) National Climatic Data Center. http://www.ncdc.noaa.gov/. Accessed 16 Jan 2020
National Oceanic and Atmospheric Administration (2020) Tides and Currents. https://tidesandcurrents.noaa.gov/. Accessed 3 Mar 2020
Natural Resource Council (2014) Reducing coastal risk on the East and Gulf Coasts. The National Academies Press, Washington, DC
Nicholls RJ, Leatherman SP (1995) Sea-level rise and coastal management. In: McGregor DFM, Thompson DA (eds) Geomorphology and land management in a changing environment. Wiley, New York, NY
Nyman JA, Chabreck RH (2012) Managing coastal wetlands for wildlife. In: Silvy NJ (ed) The wildlife techniques manual, vol 2, 7th edn. The Johns Hopkins University Press, Baltimore, MD, pp 133–156
Nyman JA, DeLaune RD, Roberts HH, Patrick WH Jr (1993) Relationship between vegetation and soil formation in a rapidly submerging coastal marsh. Marine Ecology Progress Series 96:269–279
Nyman JA, Walters RJ, Delaune RD, Patrick WH (2006) Marsh vertical accretion via vegetative growth. Estuarine, Coastal and Shelf Science 69:370–380
Osland MJ, Enwright NM, Stagg CL (2014) Freshwater availability and coastal wetland foundation species: Ecological transitions along a rainfall gradient. Ecology 95:2789–2802
Osland MJ, Enwright NM, Day RH, Gabler CA, Stagg CL, Grace JB (2016) Beyond just sea-level rise: considering macroclimatic drivers within coastal wetland vulnerability assessments to climate change. Global Change Biology 22:1–11
Osland MJ, Griffith KT, Larriviere JC, Feher LC, Cahoon DR, Enwright NM, Oster DA, Tirpak JM, Woodrey MS, Collini R, Baustian JJ, Breithaupt JL, Cherry JA, Conrad JR, Cormier N, Coronado-Molina CA, Donoghue JF, Graham SA, Harper JW, Hester MW, Howard RJ, Krauss KW, Kroes DE, Lane RR, McKee KL, Mendelsshon IA, Middleton BA, Moon JA, Piazza SC, Rankin NM, Sklar FH, Steyer GD, Swanson KM, Swarzenski CM, Vervaeke WC, Willis JM, Wilson KV (2017) Assessing coastal wetland vulnerability to sea-level rise along the northern Gulf of Mexico coast: gaps and opportunities for developing a coordinated regional sampling network. PLoS ONE 12:e0183431
Osland MJ, Gabler CA, Grace JB, Day RH, McCoy ML, McLeod JL, From AS, Enwright NM, Feher LC, Stagg CL, Hartley SB (2018) Climate and plant controls on soil organic matter in coastal wetlands. Global Change Biology 24:5361–5379
Osland MJ, Grace JB, Guntenspergen GR, Thorne KM, Carr JA, Feher LC (2019) Climatic controls on the distribution of foundation plant species in coastal wetlands of the conterminous United States: Knowledge gaps and emerging research needs. Estuaries and Coasts 42:1991–2003
Osland MJ, Feher LC, Anderson GH, Vervaeke WC, Krauss KW, Whelan KRT, Balentine KM, Tiling-Range G, Smith TJ III, Cahoon DR (2020) A tropical cyclone-induced ecological regime shift: mangrove conversion to mudflat in Florida's Everglades National Park (Florida, USA). Wetlands 40:1445–1458
Osland MJ, Stevens PW, Lamont MM, Brusca RC, Hart KM, Waddle JH, Langtimm CA, Williams CM, Keim BD, Terando AJ, Reyier EA, Marshall KE, Loik ME, Boucek RE, Lewis AB, Seminoff JA (2021) Tropicalization of temperate ecosystems in North America: The northward range expansion of tropical organisms in response to warming winter temperatures. Global Change Biology 27:3009–3034
Osorio RJ, Linhoss A, Dash P (2020) Evaluation of marsh terraces for wetland restoration: a remote sensing approach. Water 12:336
Paine JG (1993) Subsidence of the Texas coast: Inferences from historical and late Pleistocene sea levels. Techtonophysics 222:445–458
Pinheiro J, Bates D, Debroy S, Sarkar D (2021) nlme: Linear and nonlinear mixed effects models. R package version 3.1–152. https://CRAN.R-project.org/package=nlme
R Core Team (2019) R: A language and environment for statistical computing. R Foundation for Statistical Computing, Vienna, Austria. http://www.R-project.org/
Ramage JK, Shah SD (2019) Cumulative compaction of subsurface sediments in the Chicot and Evangeline aquifers in the Houston-Galveston region, Texas: U.S. Geological Survey data release. https://doi.org/10.5066/P9YGUE2V
Rasser MK, Fowler NL, Dunton KH (2013) Elevation and plant community distribution in a microtidal salt marsh of the western Gulf of Mexico. Wetlands 33:575–583
Reed DJ (2002) Sea-level rise and coastal marsh sustainability: Geological and ecological factors in the Mississippi delta plain. Geomorphology 48:233–243
Ridd P, Sandstrom MW, Wolanski E (1988) Outwelling from tropical tidal salt flats. Estuarine, Coastal and Shelf Science 26:243–253
Saintilan N, Khan NS, Ashe E, Kelleway JJ, Rogers K, Woodroffe CD, Horton BP (2020) Thresholds of mangrove survival under rapid sea level rise. Science 368:1118–1121
Seneviratne SI, Zhang X, Adnan M, Badi W, Dereczynski C, Di Luca A, Ghosh S, Iskandar I, Kossin J, Lewis S, Otto F, Pinto I, Satoh M, Vicente-Serrano SM, Wehner M, Zhou B (2021) Weather and climate extreme events in a changing climate. In: Masson-Delmotte V, Zhai P, Pirani A, Connors SL, Péan C, Berger S,

Caud N, Chen Y, Goldfarb L, Gomis MI, Huang M, Leitzell K, Lonnoy E, Matthews JBR, Maycock TL, Waterfield T, Yelekçi O, Yu R, Zhou R (eds) Climate change 2021: the physical science basis. Contribution of Working Group I to the Sixth Assessment Report of the Intergovernmental Panel on Climate Change. Cambridge University Press, Cambridge, UK

Sherrod CL, McMillan C (1985) The distributional history and ecology of mangrove vegetation along the northern Gulf of Mexico coastal region. Contributions in Marine Science 28:129–140

Simpson GL (2018) Modelling palaeoecological time series using generalized additive models. Frontiers in Ecology and Evolution. https://doi.org/10.3389/fevo.2018.00149

Simpson GL (2021) gratia: Graceful 'ggplot'-based graphics and other functions for GAMs fitted using 'mgcv.' R package version 0.5–1. https://CRAN.R-project.org/package=gratia

Stagg CA, Osland MJ, Moon JA, Hall CT, Feher LC, Jones WR, Couvillion BR, Hartley SB, Vervaeke WC (2020) Quantifying hydrologic controls on local- and landscape-scale indicators of coastal wetland loss. Annals of Botany 125:365–376

Stagg CL, Osland MJ, Moon JA, Feher LC, Laurenzano C, Lane TC, Jones WR, Hartley SB (2021) Extreme precipitation and flooding contribute to sudden vegetation dieback in a coastal salt marsh. Plants 10:1841

Steyer GD (1993) Sabine Terracing Project Final Report, DNR project number 4351089. Louisiana Department of Natural Resources, Coastal Resources Division, Baton Rouge, LA

Swanson K (2020) Sentinel Site Annual Report- Heron Flats, Aransas National Wildlife Refuge. Mission Aransas National Estuarine Research Reserve, Port Aransas, TX

Sweet WV, Kopp RE, Weaver CP, Obeysekera J, Theiler ER, Zervas C (2017) Global and regional sea-level rise scenarios for the United States, NOAA Technical Report NOS CO-OPS 083. National Oceanic and Atmospheric Administration, Silver Spring, MD

Texas Comptroller Office (2020) Gulf Coast Region 2020 Regional Report, Gulf Coast Region Snapshot. https://comptroller.texas.gov/economy/economic-data/regions/2020/gulf-coast.php. Accessed 20 Jan 2021

Törnqvist TE, Jankowski KL, LI Y, González JL (2020) Tipping points of Mississippi Delta marshes due to accelerated sea-level rise. Sci Adv 6:aaz5512

Torsten H, Bretz F, Westfall P (2021) multcomp: Simultaneous inference in general parametric models. R package version 1.4–16. https://CRAN.R-project.org/package=multcomp

Turner RE, Streever B (2002) Approaches to coastal wetland restoration: northern Gulf of Mexico. Kugler Publications, Hague, Netherlands

Weaver CA, Armitage AR (2018) Nutrient enrichment shifts mangrove height distribution: Implications for coastal woody encroachment. PLoS ONE 13:e0193617

Webb EL, Friess DA, Krauss KW, Cahoon DR, Guntenspergen GR, Phelps J (2013) A global standard for monitoring coastal wetland vulnerability to accelerated sea-level rise. Nature Climate Change 3:458–465

Williams HFL (2010) Storm surge deposition by Hurricane Ike on the McFaddin National Wildlife Refuge, Texas: Implications for paleotempestology studies. Journal of Foraminiferal Research 40:210–219

Williams HF, Denlinger EE (2013) Contribution of Hurricane Ike storm surge sedimentation to long-term aggradation of coastal marshes in southeastern Texas and southwestern Louisiana. Journal of Coastal Research 65:838–843

Williams H, Liu K-b (2019) Contrasting Hurricane Ike washover sedimentation and Hurricane Harvey flood sedimentation in a Southeastern Texas coastal marsh. Marine Geology 417:106011

Withers K (2002) Wind-tidal flats. In: Tunnell JW, Judd FW (eds) The Laguna Madre of Texas and Tamaulipas. Texas A&M University Press, College Station, TX, pp 114–126

Wood SN (2000) Modelling and smoothing parameter estimation with multiple quadratic penalties. Journal of the Royal Statistical Society: Series B (statistical Methodology) 62:413–428

Wood SN (2017) Generalized additive models: An introduction with R, 2nd edn. CRC/Taylor & Francis, Boca Raton, FL

Wood SN (2020) mgcv: Mixed GAM computation vehicle with automatic smoothness estimation. R package version 1.8–33. https://CRAN.R-project.org/package=mgcv

Woodroffe CD, Rogers K, McKee KL, Lovelock CE, Mendelssohn IA, Saintilan N (2016) Mangrove sedimentation and response to relative sea-level rise. Annual Review of Marine Science 8:243–266

Yao Q, Liu K, Williams H, Joshi S, Bianchette TA, Ryu J, Dietz M (2020) Hurricane Harvey storm sedimentation in the San Bernard National Wildlife Refuge, Texas: fluvial versus storm surge deposition. Estuar Coasts 43:971–983

Yeates AG, Grace JB, Olker JH, Guntenspergen GR, Cahoon DR, Adamowicz S, Anisfield SC, Barrett N et al (2020) Hurricane Sandy effects on coastal marsh elevation change. Wetlands 43:1640–1657

Zedler JB (1982) The ecology of southern California coastal salt marshes: a community profile, U.S. Fish and Wildlife Service report FWS/OBS-81/54. U.S. Fish and Wildlife Service, Biological Services Program, Washington, DC